Supplement of Ocean Sci., 15, 1247–1266, 2019
https://doi.org/10.5194/os-15-1247-2019-supplement

Ocean Science Open Access EGU

Supplement of

Synoptic-scale variability of surface winds and ocean response to atmospheric forcing in the eastern austral Pacific Ocean

Iván Pérez-Santos et al.

Correspondence to: Iván Pérez-Santos (ivan.perez@ulagos.cl)

Introduction

The supplementary figures include the comparison of surface wind data components (u and v) from a buoy and different Navy lighthouses (NLH) located on the coast of Patagonia, with the satellite wind products ASCAT and QuikSCAT and the ERA5 reanalysis climate data set (Figs. S1, S2, S3, S4, and S5). The period from 2017–2018 was used for the analysis between the buoy and ERA5, and the years 2009–2011 and 2014 were used in the case of the NLH wind data. To quantify the statistical relationship between the data sets, a Taylor diagram (Taylor, 2001) was applied.

Additional EOF analysis was incorporated into the supplementary section to demonstrate the influence of LAP and HAP structures in the EOF eigenvector patterns (Figs. S6-S8). The EOF was carried out using the same ERA5 reanalysis data set but covering a larger area as shown in Fig.3 of the manuscript.

Studies of nighttime heatwave events were added to this section to demonstrate the relationship between atmospheric pressure systems, meridional winds, and surface air temperature in the generation of surface air temperature night-time maxima (Fig. S9).

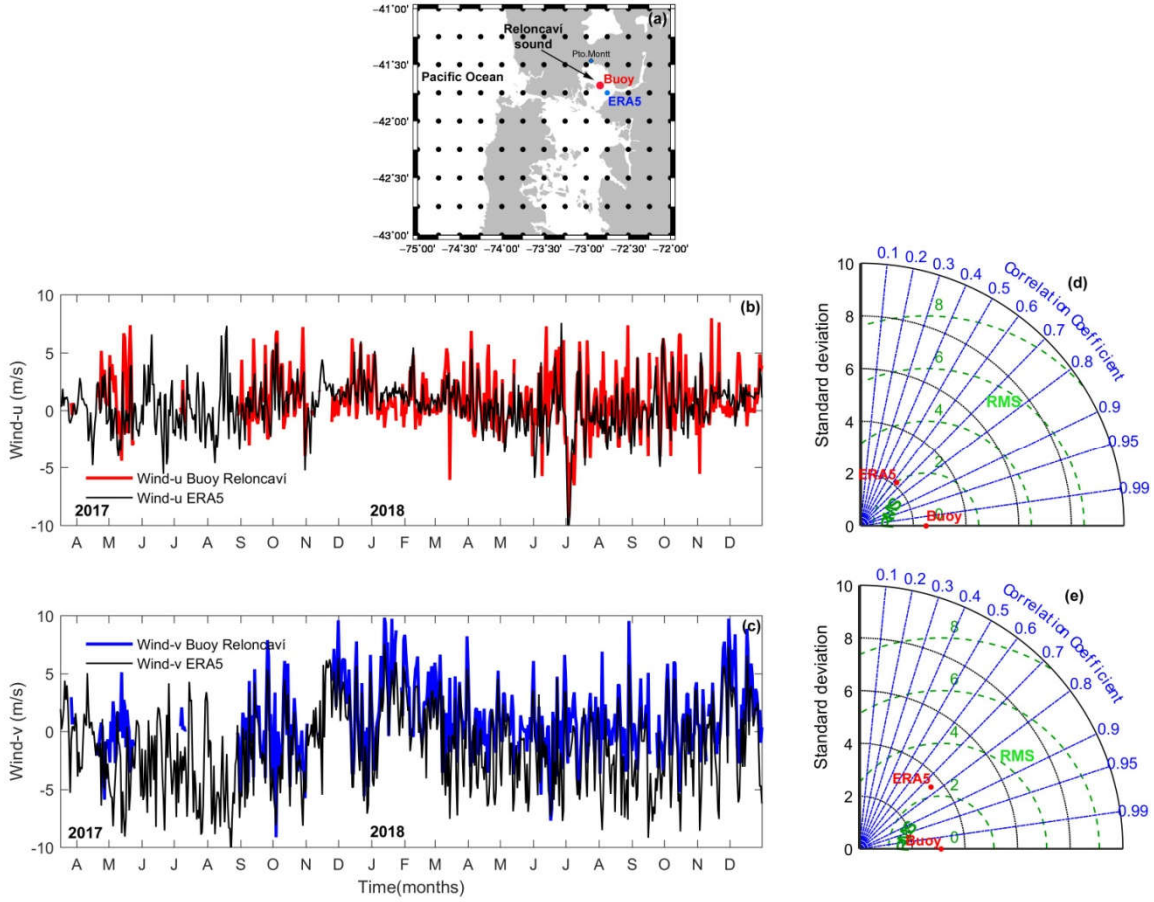

Figure S1. (**a**) Map showing the grid data from the ERA5 reanalysis (black dots) and the position of the oceanographic buoy moored in Reloncaví Sound. (**b** and **c**) Time series of the wind components u and v, and (**d** and **e**) Taylor diagrams correlating wind data from the buoy with the ERA5 reanalysis. In (**d** and **e**) the blue lines represent the correlation coefficient, the green lines represent the root mean square error, and the black lines represent the standard deviation.

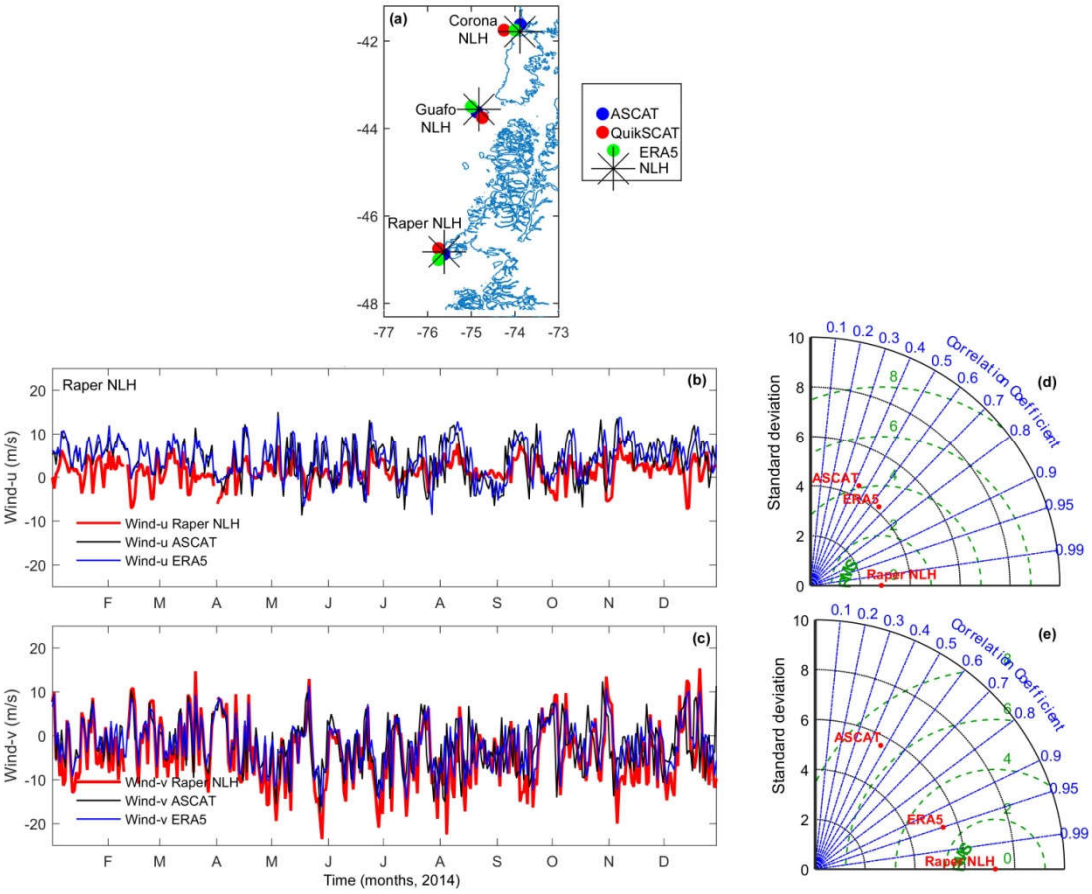

Figure S2. (**a**) Map showing the positions of the different Navy lighthouses (NLH), the ASCAT satellite wind product, and the ERA5 reanalysis grid points closest to the NLH. (**b** and **c**) Time series of wind components u and v and (**d** and **e**) Taylor diagrams correlating wind data from Raper NLH with the ASCAT data and the ERA5 reanalysis. In (**d** and **e**) the blue lines represent the correlation coefficient, the green lines are the root mean square error, and the black lines are the standard deviation.

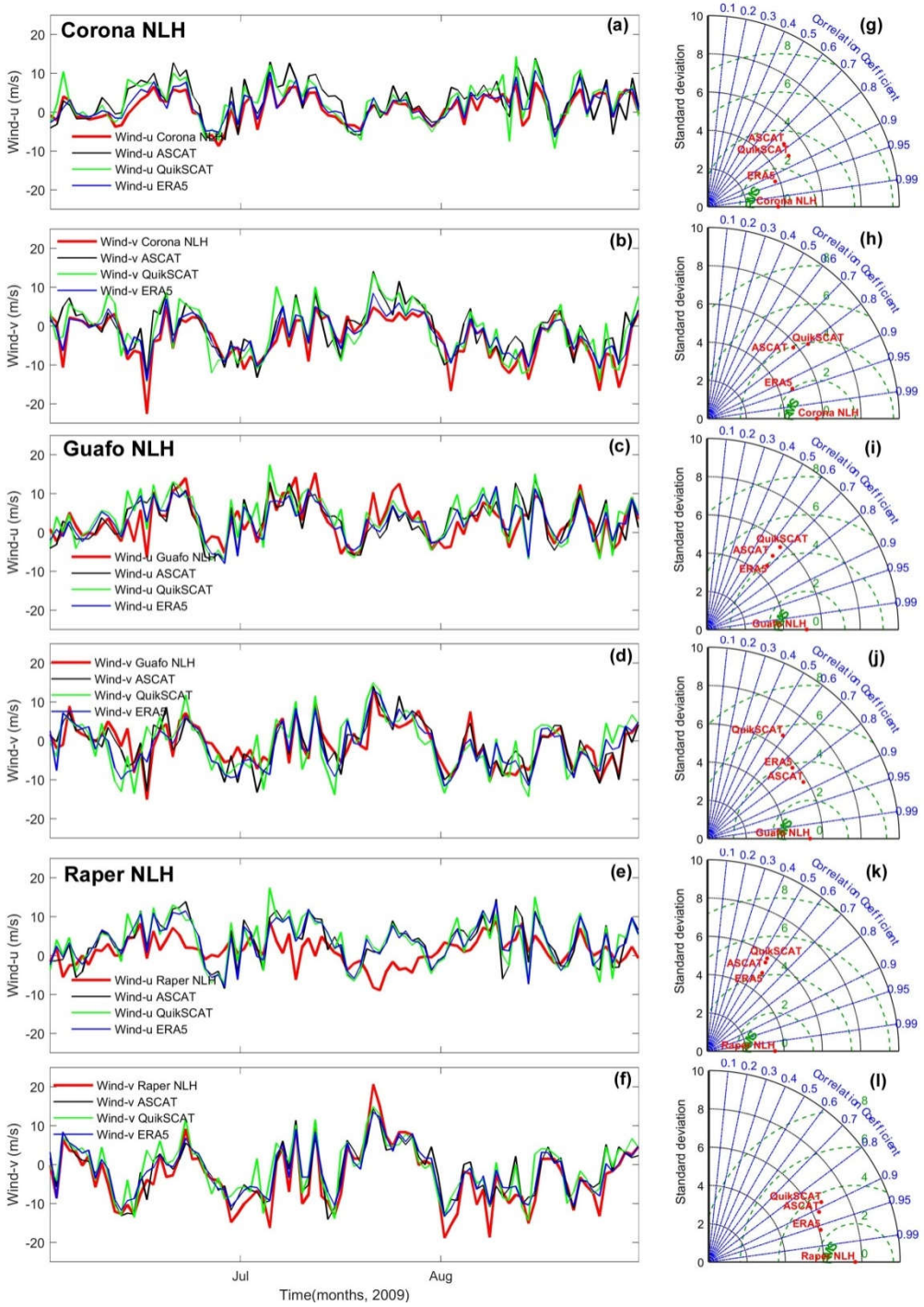

Figure S3. (**a**–**f**) Time series of wind components u and v from different NLH with the satellite wind products (ASCAT and QuikSCAT) and the ERA5 reanalysis. (**g**–**l**) Taylor diagrams in which blue lines represent the correlation coefficient, the green lines are the root mean square error, and the black lines are the standard deviation.

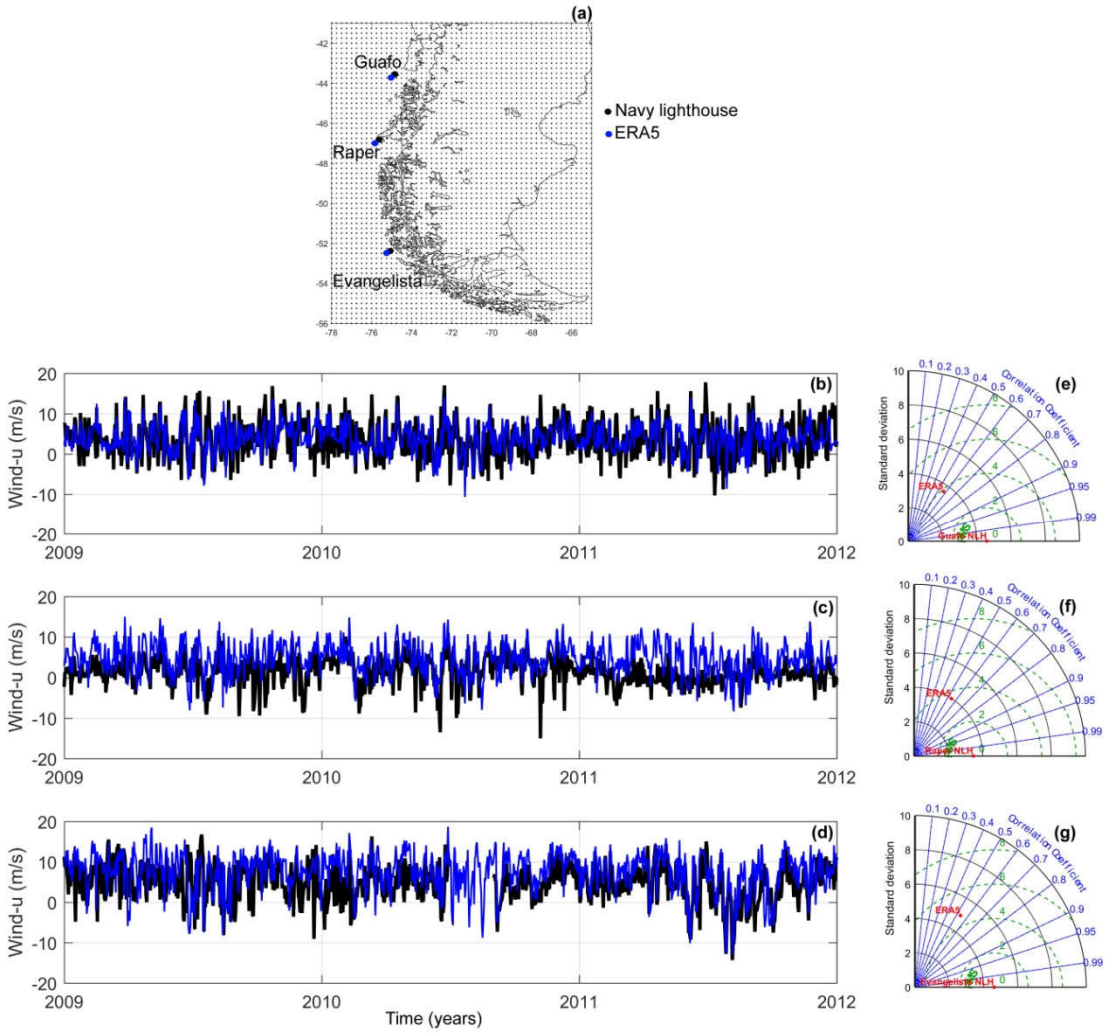

Figure S4. (**a**) Map showing the positions of the different NLH and the ERA5 reanalysis grid points closest to the NLH. (**b**–**d**) Time series of wind components u from different NLH and the ERA5 reanalysis. (**e**–**g**) Taylor diagrams in which blue lines represent the correlation coefficient, the green lines are the root mean square error, and the black lines are the standard deviation.

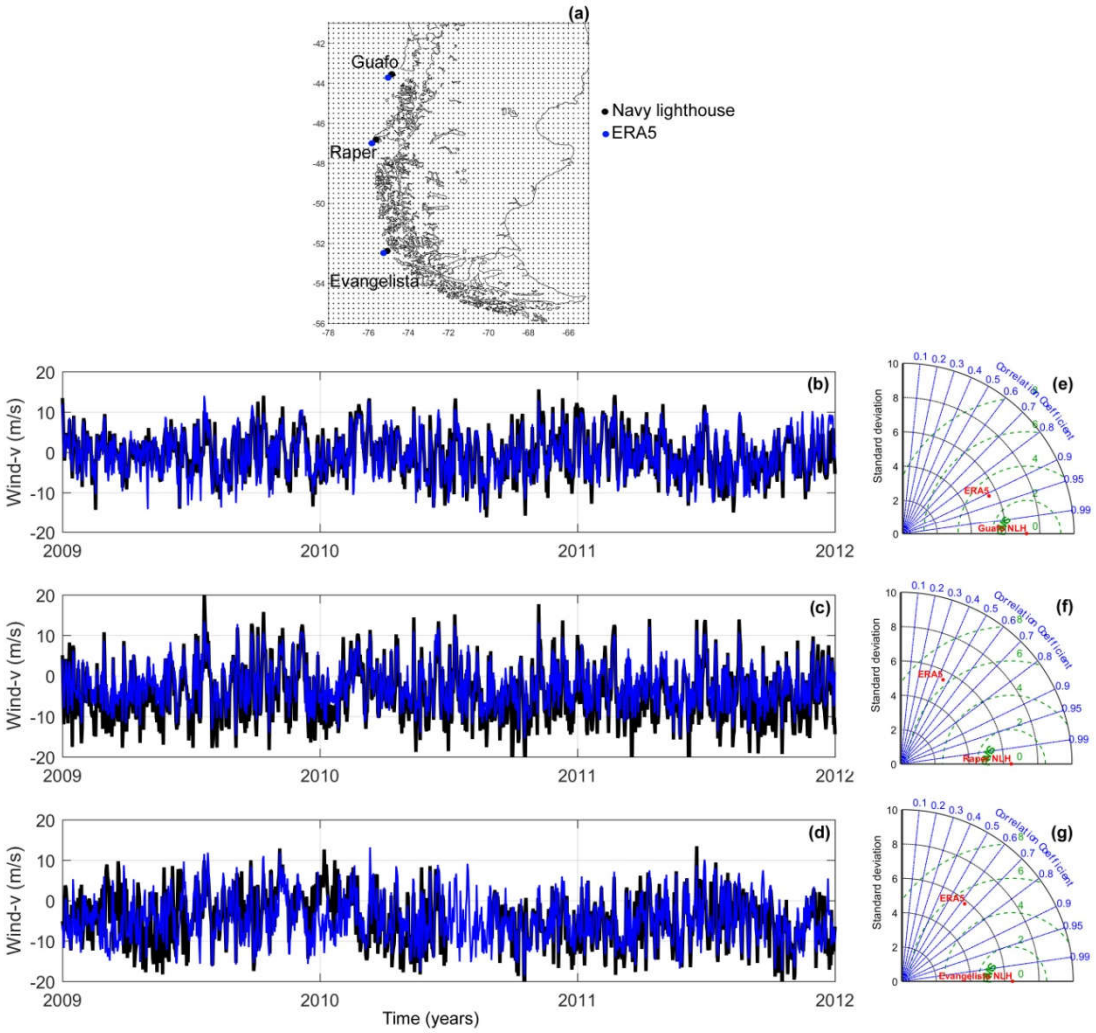

Figure S5. (**a**) Map showing the positions of the different NLH and the ERA5 reanalysis grid points closest to the NLH. (**b**–**d**) Time series of wind components v from different NLH and the ERA5 reanalysis. (**e**–**g**) Taylor diagrams in which blue lines represent the correlation coefficient, the green lines are the root mean square error, and the black lines are the standard deviation.

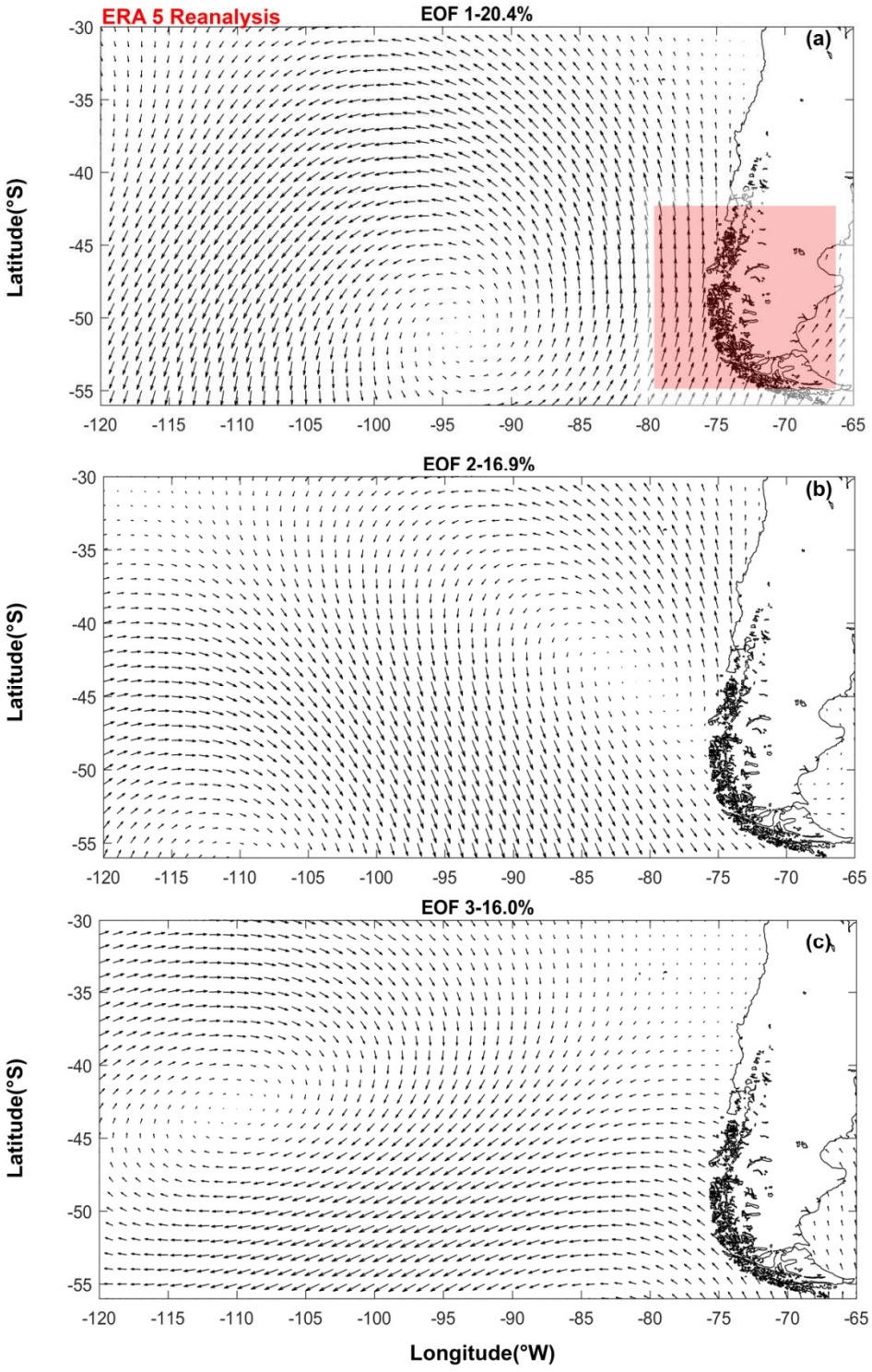

Figure S6. Eastern Austral Pacific Ocean, 1999 to 2015: normalized eigenvector patterns, from ERA5 reanalysis (**a**, **b** and **c**).The red rectangle in (**a**) indicates the study area.

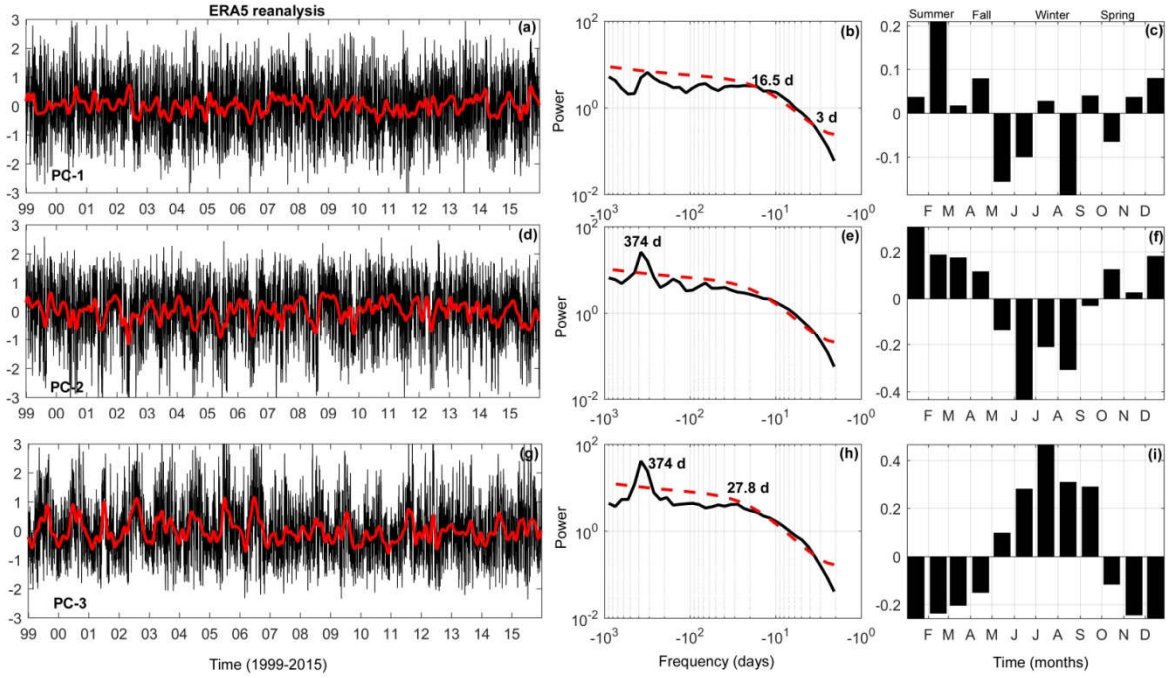

Figure S7.(**a**, **d**, and **g**) Normalized time series of the time-dependent coefficient (black lines) from the 30-day, low pass filtered time series (solid red lines). (**b**, **e**, and **h**) Global wavelet spectra (black solid lines) with 95% confidence interval (red dashed lines), and (**c**, **f**, and **i**) long term monthly mean of EOF modes from surface winds daily data of ERA5 reanalysis from 1999 to 2015: mode 1 (**a**, **b**, and **c**), mode 2 (**d**, **e**, and **f**), mode 3 (**g**, **h**, and **i**).

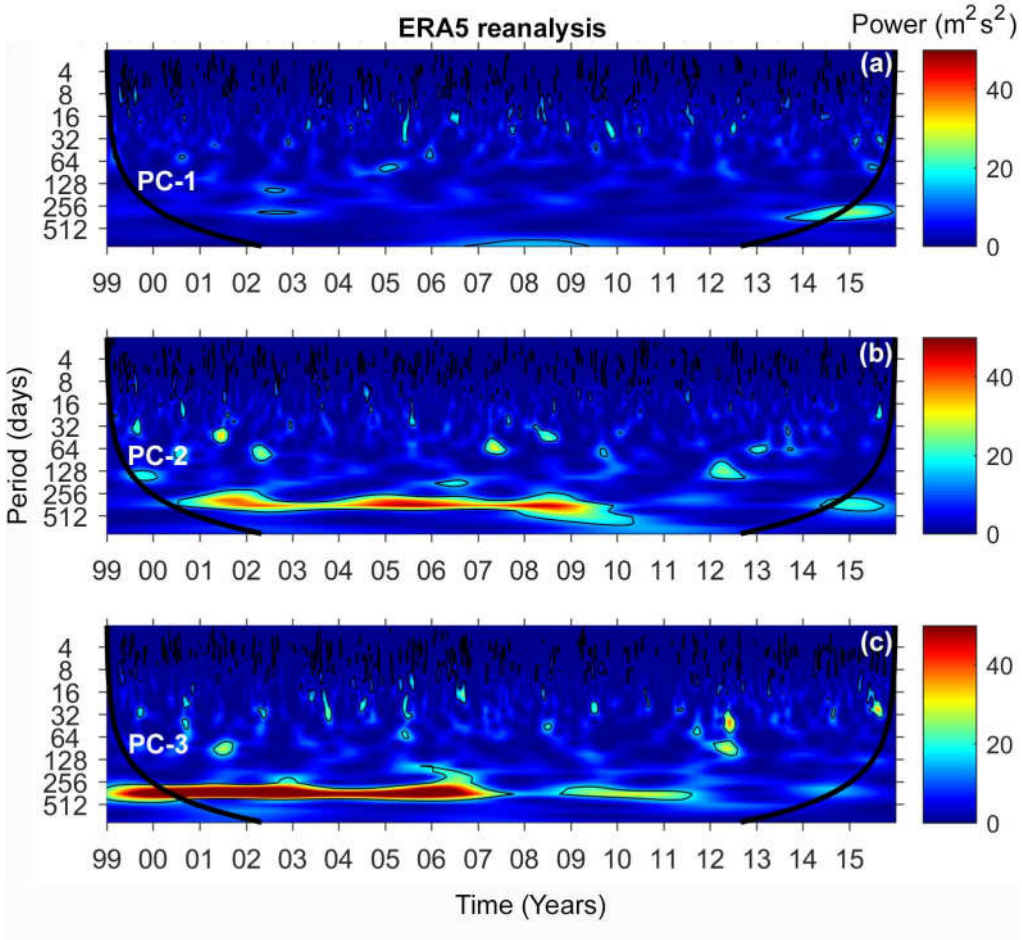

Figure S8. Morlet wavelet power spectrum applied to the three series of the EOF time-dependent coefficient from ERA5 (**a**, **b**, and **c**).The fine contour lines enclose regions of confidence levels of >95% for a red noise process with a lag 1 coefficient between 0.62 and 0.72, and the thick contour lines indicate the cone of influence. The color bar relates colors on the power spectrum.

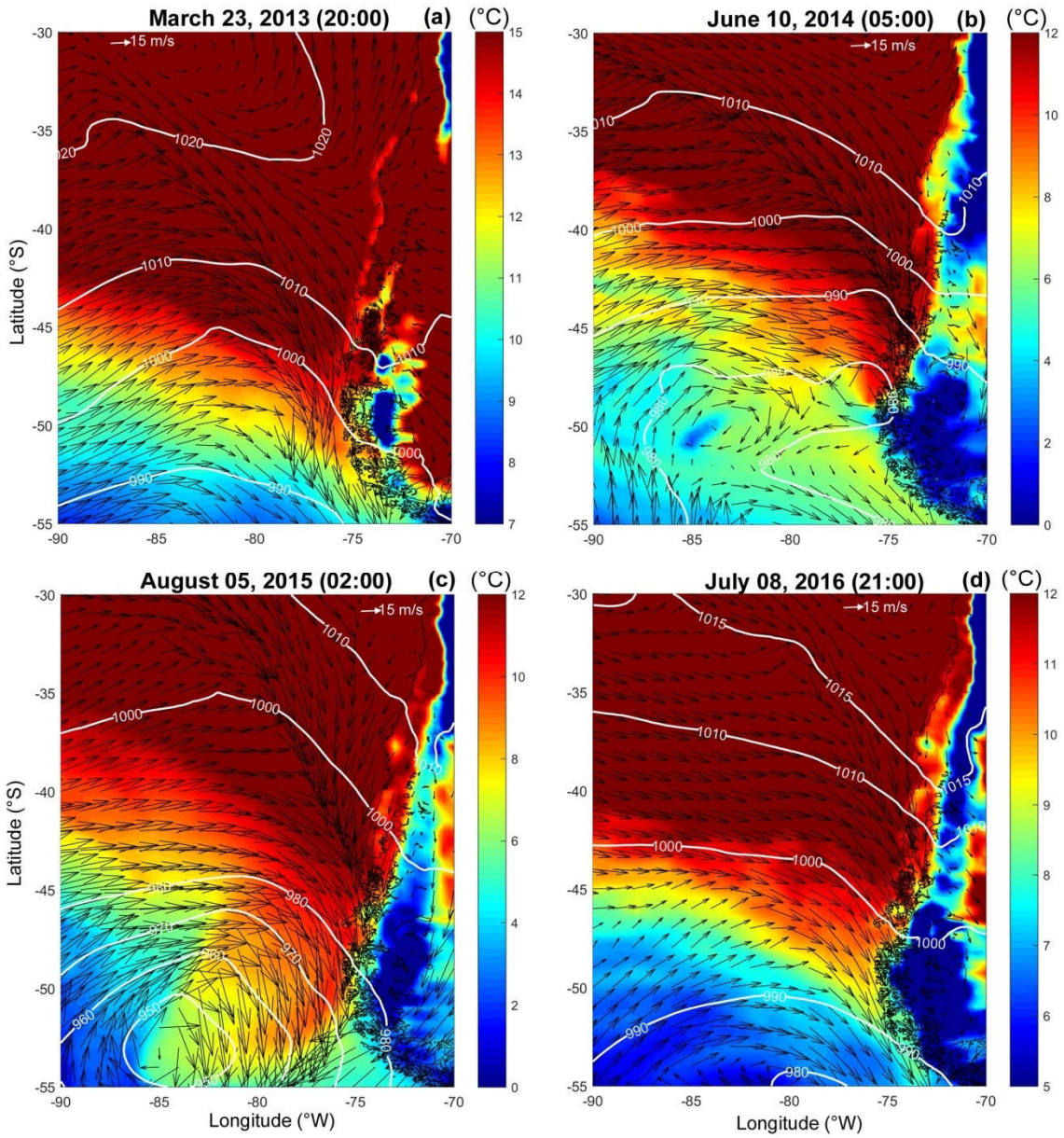

Figure S9. (**a**, **b**, **c**, and **d**) Different cases of night-time heatwave events extracted from time series presented in Fig. 13**a** and Fig. 13**c**, using the hourly data of ERA5 reanalysis. The white contour lines represent the atmospheric pressure (mbar) values and the black arrows indicatethe wind directions and intensity (m s^{-1}). The color bars relate colors to surface air temperature (°C).

Reference

Taylor, K. E.: Summarizing multiple aspects of model performance in a single diagram, J. Geophys. Res., 106, 7183–7192, doi:10.1029/592 2000JD900719, 2001.